



Deposited via The University of Sheffield.

White Rose Research Online URL for this paper:

<https://eprints.whiterose.ac.uk/id/eprint/175277/>

Version: Published Version

Article:

Güleç, F., Riesco, L.M.G., Williams, O. et al. (2021) Hydrothermal conversion of different lignocellulosic biomass feedstocks – effect of the process conditions on hydrochar structures. *Fuel*, 302. 121166. ISSN: 0016-2361

<https://doi.org/10.1016/j.fuel.2021.121166>

Reuse

This article is distributed under the terms of the Creative Commons Attribution (CC BY) licence. This licence allows you to distribute, remix, tweak, and build upon the work, even commercially, as long as you credit the authors for the original work. More information and the full terms of the licence here:

<https://creativecommons.org/licenses/>

Takedown

If you consider content in White Rose Research Online to be in breach of UK law, please notify us by emailing eprints@whiterose.ac.uk including the URL of the record and the reason for the withdrawal request.



Full Length Article

Hydrothermal conversion of different lignocellulosic biomass feedstocks – Effect of the process conditions on hydrochar structures

Fatih Güleç^{a,*}, Luis Miguel Garcia Riesco^a, Orla Williams^a, Emily T. Kostas^b, Abby Samson^c, Edward Lester^a

^a Advanced Materials Research Group, Faculty of Engineering, University of Nottingham, Nottingham NG7 2RD, UK

^b Advanced Centre of Biochemical Engineering, Bernard Katz Building, University College London, Gower Street, London WC1H 6BT, UK

^c Department of Mechanical Engineering, University of Sheffield, Sheffield S3 7RD, UK



ARTICLE INFO

Keywords:

Hydrothermal conversion
Hydrochar
Bioenergy
Lignocellulosic Biomass
Displacement

ABSTRACT

Five biomass feedstocks (Coffee residues, Rice waste, Whitewood, Zilkha black, and Lignin) were hydrothermally processed in a semi-continuous flow rig using 9 different processing conditions (75, 150, 250 °C, and 1, 50, 240 bar). Solid residues produced at low temperature (<150 °C) did not show significant structural changes. At more severe conditions, structural changes could be linked to the lignocellulosic composition and divided into three categories: (i) biomass with higher hemicellulose-cellulose and lower cellulose-lignin structures, (ii) lower hemicellulose-cellulose and higher cellulose-lignin structures, and (iii) only cellulose-lignin structures. Both hemicellulose and cellulose structures in category (i) and (ii) were successfully degraded under subcritical conditions (250 °C and 50 bar) to produce hydrochar with higher lignin content. Biomasses with higher levels of lignin did not show the same degree of transformation. Category (i) produced a low hydrochar yield (39 wt%) due to the degradation of higher hemicellulose-cellulose structures. Category (ii) had higher hydrochar yields (58–62 wt%) due to the lower amount of cellulose and hemicellulose. Category (iii) had the highest hydrochar yields (73–90 wt%) thanks to the lack of hemicellulose and lower cellulosic structures. A novel concept called “displacement”, based on a thermogravimetric profiling method, was used to quantify changes in the pyrolysis behaviour of the hydrochar compared to the original feedstock. The degree of “displacement” correlated with hydrochar yield and reactivity, the highest level of displacement was observed with category (i- higher hemicellulose-cellulose biomasses) while the lowest displacement was observed with category (iii- higher lignin biomasses). This novel technique could be used to quantify the effects of hydrothermal treatment on any given biomass.

1. Introduction

Thermal and biological biomass processing technologies such as pyrolysis, combustion, hydrothermal processes (liquefaction, gasification, and carbonisation) and biochemical conversion have all been identified as pathways to decrease CO₂ emissions and reach the 2 °C climate target [1]. Biomass is defined as inexpensive, clean, and environmentally friendly energy sources [2,3] and an integral part of the global carbon cycle [4]. However, there are several obstacles to the full commercialisation of bioenergy and bioproducts via these technologies, which include the resourcing of biomass, inadequate biomass refinery technologies, a lack of cost-competitive bioproducts and a limited and/or unstable supply of biofuels and bioproducts [5]. Furthermore, the

chemical and biological variations in different types of biomass can result in significant changes in characteristics (grinding, handling, composition etc) that can hinder the commercialisation of these technologies [6–8]. Lignocellulosic biomass feedstocks are defined as one of the crucial renewable energy sources thanks to its availability, high energy content, and reactivity. The lignocellulosic biomass chars can be produced by pyrolysis, torrefaction, and hydrothermal processes [9]. The lignocellulosic biomasses are composed of hemicellulose, cellulose, and lignin in addition to a small quantity of extractives and ashes [10]. Although the composition of lignocellulosic biomass varies according to the type, location, maturity, and climate conditions, on average it consists of about 15–30% of hemicellulose, 40–60% of cellulose, and 10–25% of lignin [11].

* Corresponding author.

E-mail addresses: Fatih.Gulec1@nottingham.ac.uk, Gulec.Fatih@outlook.com (F. Güleç).

<https://doi.org/10.1016/j.fuel.2021.121166>

Received 7 April 2021; Received in revised form 27 May 2021; Accepted 30 May 2021

Available online 15 June 2021

0016-2361/© 2021 The Authors. Published by Elsevier Ltd. This is an open access article under the CC BY license (<http://creativecommons.org/licenses/by/4.0/>).

Hydrothermal processing is one of the most promising technologies, as it can use the high inherent moisture of biomass to its advantage [12]. For other processing techniques, such as pyrolysis and combustion, the high moisture content needs to be removed which requires a significant amount of energy for drying processes. In contrast, hydrothermal conversion of biomass in hot-compressed water is a viable, scalable, and energy-efficient thermo-chemical route for converting biomass into a synthetic solid, liquid, or gaseous fuels and chemicals [13]. In hydrothermal treatments, water can be a solvent, a reactant and/or a catalyst in the hydrolysis reactions. The process also leads to by-products that can be used for power generation and the recovery of useful nutrients [14]. In this process, the biomass conversion is carried out by several complex reactions depending on the physical properties of the water, which are usually manipulated changing the temperature, pressure, and contact time of the water-biomass in order to obtain the desired products. The hydrothermal conversion is therefore classified into three processes namely carbonisation, liquefaction and gasification depending on the severity of the operating conditions [15–18].

Hydrothermal gasification (HTG, >350 °C) is carried out near-critical or above-critical conditions to produce a synthetic fuel gas (syngas), which is rich in CH₄, H₂, CO₂, and CO depending on experimental conditions [15]. Depending on the biomass, the syngas may contain a significant amount of undesirable impurities such as sulphur compounds (SO₂), nitrogen compounds (NH₃ and HCN), hydrogen halides (HCl and HF) [16]. Hydrothermal liquefaction (HTL, 250–370 °C, 50–240 bar) is the wet processing route for high moisture biomasses to produce of a liquid fuel (bio-crude) [15] which is similar to petroleum crude and can be upgraded to a range of petroleum-derived fuel products [17]. Since HTL involves the direct conversion of the biomass into bio-crude in the presence of a solvent, it eliminates the high drying costs [18–20]. Hydrothermal carbonization (HTC, 180–250 °C, 15–40 bar) is a thermochemical process for the pre-treatment of high moisture content biomass to make it viable in for energy production [17,21,22]. HTC uses relatively low temperatures and is suitable for any kind of biomass feedstock [23]. HTC can convert lignocellulosic materials into solid hydrochar, which have better physicochemical characteristics than raw biomass feedstocks [24] and also produce liquid products that contain organic and inorganic value-added chemicals [25]. The HTC hydrochars exhibits lower O/C and H/C ratios compared to dry torrefaction and turn into more lignin or coal type materials [26]. HTC hydrochars can be used in a wide range of processes such as soil amendment [27] CO₂ capture [28] nanoparticles (for making composites) [29] energy production [30] water purification [31] thanks to their physicochemical properties [32]. Although the lab-scale research on HTC of various biomass feedstocks has been recently progressed and provided significantly promising results, the HTC process needs further investigations in terms of process and reactor types, biomass feedstocks, and conditions due to the complex reaction mechanisms and operational barriers to make this technology as a commercial technology [25]. For example, a continuous HTC process would be one of the key components for a potential industrial application of HTC, as most HTC research have been carried out in batch [25].

In this study, the hydrothermal conversion of five different lignocellulosic biomass feedstocks (Coffee residues, Whitewood, Rice waste, Zilkha black, and Lignin) was investigated in a semi-continuous process at different temperatures (75, 150, and 250 °C) and pressures (1, 50 and 240 bar) to produce hydrochars. Each hydrochar sample was characterised in a Thermogravimetric Analyser (TGA) using a slow pyrolysis methodology to identify the effects of hydrothermal treatments on hydrochar structures using thermal decomposition behaviours. Additionally, a new method called “displacement” was shown to provide quantitative information about the impact of hydrothermal treatment on the lignocellulosic composition of biomass feedstocks. This method has been previously used as a fingerprint technique for biomass identification as it can quantify hemicellulose, cellulose and lignin levels present in any type of biomass [33].

2. Material and Methods

The effects of the hydrothermal conversion process conditions on the hydrochar structures were investigated using five different biomass feedstocks namely Coffee residues (CR, as an industrial waste, obtained from spent aluminum capsules used in certain domestic coffee machines), Whitewood (WW, as a forest waste, obtained from sawdust of white wood), Rice waste (RW, as a food waste, obtained from rice pellets), and Zilkha black (steam exploded white wood pellets) and Lignin (ZB and LG as high carbon ratio materials, obtained from Zilkha Black® pellets and Lignin pellets). These feedstocks have been selected due to their abundance in environment and commercial availability, as well as their potential to produce hydrochars having different properties [6,34,35]. Zilkha was chosen as it represents a wood based, lignocellulosic feedstock but one that has already been pretreated/upgraded using thermal methods. The biomass feedstocks (CR, WW, RW, ZB and LG) were firstly ground into a powder and sieved in particle sizes of 200–1000 µm in a sieve shaker for 15 min using the standard method of EN ISO 17827-2:2016 – *Solid biofuels – Determination of particle size distribution for uncompressed fuels – Part 2: Vibrating screen method using sieves with aperture of 3,15 mm and below* [36,37].

2.1. Hydrothermal processing

The biomass feedstocks (CR, WW, RW, ZB, and LG) were hydrothermally processed using a semi-continuous flow rig shown in Fig. 1. The operation of the rig consists of a semi-continuous reactor that works by preloading a biomass sample inside a 100 µm mesh and processing using a semi-continuous hydrothermal flow. The feed stream (distilled water) TK-101 is pumped using a high pressure Gilson HPLC pump (P-101) and preheated to the desired temperature using a Watlow cartridge heater (E-101). The preheated water stream flows into the reactor (R-101) from the bottom, where the reaction starts with the effects of matter and energy transfer. The enriched stream leaves the reactor and passes through a filter (F-101) of 100 µm that retains any solids that could potentially have flowed out the top of the reactor. After the filter, the resulting products are cooled in a heat exchanger (E-102) with a stream of fresh water. Finally, the product stream goes through a back-pressure regulator (BPR) which pressurizes the whole system and the outflow is collected after the BPR (TK-102). The main focus of this study was the residual solids in the reactor rather than the contents of the liquid effluent.

The hydrothermal conversion of CR, WW, RW, ZB and LG were investigated at low to medium temperatures (75, 150, and 250 °C) and pressures (1, 50, and 240 bar), as seen in

Fig. 2, to establish the optimal conditions for hydrochar production at low temperatures. Approximately 5.0 g of each biomass feedstock (CR, WW, RW, ZB, and LG) was placed between two layers of sieves (100 µm) into the steel reactor. Once pressure had been obtained, the flow rates were reduced to a minimal level (1–5 ml/min) The hydrothermal rig was then pressurised using a distilled water flow rate of 20 ml/min. The heat exchanger temperature was then set the target temperature (75, 150, and 250 °C). Once the system had stabilised at the desired conditions, the water flow rates were then introduced to the reactor with a flow rate of 20 ml/min. The total residence time of water in the reactor was determined about 1.9–2.3 min from pump to back pressure regulator. The liquid product stream was cooled to about 20–30 °C in a heat exchanger using a water stream and collected and then stored in a freezer at –18 °C for further analysis. The hydrochars were collected from the reactor and dried in an oven at 100 °C for overnight.

2.2. Char formation and analysis

The yield of hydrochar (or solid residue) after each hydrothermal conversion experiments was determined using the following equation

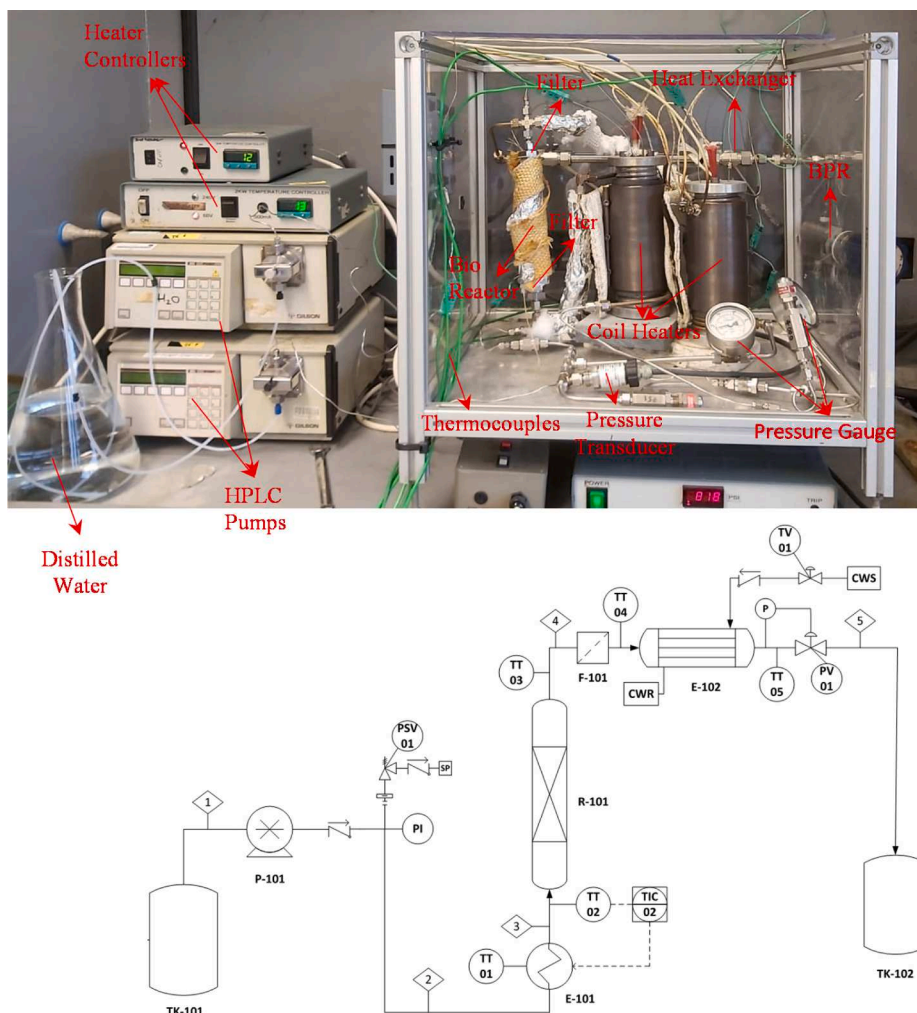


Fig. 1. Semi-continuous hydrothermal treatment process rig and flow diagram.

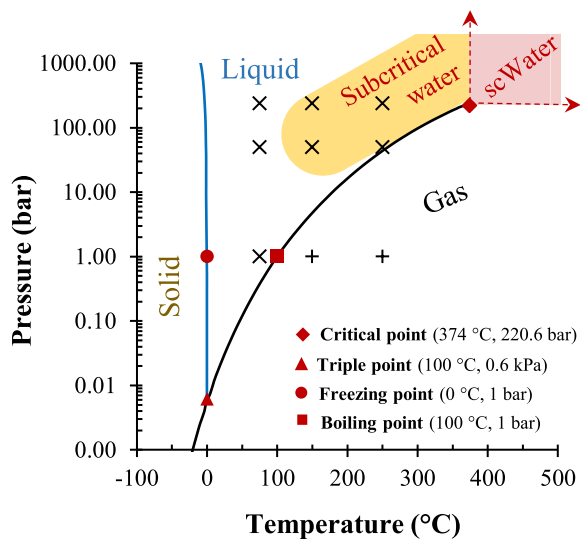


Fig. 2. A schematic phase diagram showing Pressure – Temperature for water including the near and supercritical region (scWater). Plus (+) and Cross (x) signs represent the experiments investigated under vapour and liquid conditions, respectively.

(Eq-1) [38].

$$\text{Solid residue (wt.\%)} = \frac{m_{char,dry}}{m_{biomass,dry}} * 100 \tag{1}$$

Where, $m_{char,dry}$: the dried weight of hydrochar (g) after hydrothermal conversion, $m_{biomass,dry}$: the dried weight of biomass (g) before hydrothermal conversion.

2.3. Thermogravimetric analysis

A thermogravimetric characterisation technique was used to measure the pyrolysis and then combustion behaviour of each biomass and hydrochar sample. This technique has been used to quantify components such as hemicellulose, cellulose [33]. A TA-Q500 system was loaded with approximately 15–25 mg of hydrochar (or raw biomass) using a platinum pan 4 mm deep and 10 mm in diameter. It was then heated from ambient temperature to 900 °C with a heating rate of 5.0 °C/min under N₂ flow rate of 100 ml/min and held at this temperature for about 5 min. N₂ was then replaced by air (to combust the fixed carbon) with a flow rate of 100 ml/min at 900 °C for a further 10 min [33]. The devolatilization behaviours of the biomass feedstocks and hydrochars were identified using the thermogravimetric (TG) and differential thermogravimetric (dW/dt) curves [39]. The fuel ratio was defined as the ratio of fixed carbon to volatile matter (dry ash free basis) for each biomass and hydrochar. Based on this technique, we propose a new method called “displacement” to characterize the impact of hydrothermal treatment. Displacement was determined with the global sum of all

absolute value of the differences between the original and experimental DTG profiles as defined in Eq-2.

$$\text{Displacement} = \sum_{T=25^{\circ}\text{C}}^{T=900^{\circ}\text{C}} \left(\left| \left(\frac{dw}{dt} \right)_{bf,T} - \left(\frac{dw}{dt} \right)_{hc,T} \right| \right) \quad (2)$$

Where, T is the temperature of thermal decomposition (25–900 °C), $(dw/dt)_{bf,T}$ and $(dw/dt)_{hc,T}$ are the weight loss rate of biomass feedstocks and hydrochars at the specific temperatures in the thermal degradation process. Displacement is essentially a relative measurement and can be applied to any biomass and resultant char. A large displacement number means a large change in pyrolysis behaviour and this relates back to changes in organic composition [33,40]. These displacement calculations are based on the dW/dt profiles shown in Fig. 7,9,10,12 and 13. In essence, if the hydrochars profile is a close match to the original biomass then values of 1000–2000 tend to result. If the profiles show a marked difference in terms of in peak position (on the x-axis) or shape, then values of 5000–7000 tend to be seen.

3. Results and Discussions

3.1. Characterisation of feedstocks

Proximate analysis of the lignocellulosic biomass feedstocks (LG, ZB, WW, RW, and CR) is presented in Figs. 3 and 4. Among these biomass feedstocks, the LG has the highest FC (~34 wt%) and lowest volatile matter (~65 wt%) ratios and ZB follow as second with the ~24 wt% of fixed carbon and ~75 wt% of volatile matter. WW and CR demonstrate relatively similar ratios ~15 wt% of fixed carbon and ~83 wt% of volatile matter with a low ash content (< ~2 wt%). However, RW has a relatively high ash content (~15 wt%) compared to the others. Furthermore, LG has the highest fuel ratio (0.52), while CR and WW both have the lowest fuel ratio at 0.19.

The lignocellulosic biomass consists of lignin (15–35%, non-carbohydrate source), cellulose and hemicellulose (carbohydrate sources), and potentially lipids and proteins [41]. Therefore, the thermal decomposition (slow pyrolysis) of the biomass feedstocks can provide detailed information about the biomass structures such as hemicellulose (220–315 °C), cellulose (315–400 °C), and lignin (160–900 °C) structures [33,42,43]. The DTG graph in Fig. 4 demonstrates that LG and ZB provide only one strong peak at about ~330 °C, which demonstrates the high cellulose-lignin content. Furthermore, CR is the only biomass which demonstrates two clear peaks; the first one is at ~290 °C based on hemicellulose-cellulose structure and the second one is at ~330 °C based on the cellulose-lignin structures. Additionally, there is a strong tail after the second peak which indicates a high lignin content in CR. However, WW and RW provide one peak at ~322 °C (which is the

structure of cellulose-lignin) with a detectable shoulder at 280–300 °C (originating from the hemicellulose-cellulose structures of WW and RW).

3.2. Solid residue-Hydrochar formation

After the hydrothermal conversion of biomass feedstocks (CR, WW, RW, ZB, and LG), the solid residue (or hydrochar) yields were determined using Eq-1. An increase in temperature decreases the solid residue yields at any pressure for all biomass types, as shown in Fig. 5. Residual solids at temperatures up to 150 °C are quite high due to the low ratio of water-soluble components in the lignocellulosic materials. Pressure appears to have an insignificant impact on solubility at these temperatures. The water-soluble portion of the biomass disperses into the water at ~100 °C and hydrolysis starts at temperatures above 150 °C [44]. Each of the 5 biomass feedstocks consists of a different portion of water-soluble compounds at 75 °C. ZB has the highest water-soluble portion (~1314 wt%), while the other biomass feedstocks (CR, RW, WW and LG) have only ~2–7 wt% of water-soluble portions. Conversely, the ratio of hydrolysed compounds at 150 °C is ~7–15 wt% for CR while it is lower than 5 wt% for the other biomass feedstocks. Biomass starts to carbonise at temperatures of 180–250 °C [17,22,25] as the cellulose and hemicellulosic polymers disintegrate into monomers/oligomers [44].

CR has the lowest hydrochar yield (39 wt%) at 250 °C and 50–240 bar and the dW/dt results (in Fig. 4) show two clear peaks at ~290 °C and ~330 °C, which represent the higher hemicellulose-cellulose lower cellulose-lignin structures, respectively. The low hydrochar yield is due to the removal of the hemicellulose/cellulose fraction. LG, however, provides the highest hydrochar yield (87–92 wt%) at relatively severe carbonisation conditions of 250 °C and 50–240 bar due to its low solubility and lack of hemicellulose and cellulose structures. ZB is also resilient to hydrothermal treatment with a high hydrochar yield (71–76 wt%) at the same conditions. Fig. 4 shows LG has a single thermal decomposition peak at ~336 °C. Similar to LG, ZB shows substantial low molecular weight materials evolving at low temperatures (150–225 °C). This could explain why more material solubilised into the water phase for ZB, even at relatively mild conditions. It is possible that the steam explosion breaks down the cell-wall to create lower molecular weight material which is more soluble. The strong peak at ~336 °C in LG and ZB arises from large amounts of cellulose-lignin structures.

Similarly, both RW and WW produce lower hydrochar yields (58–62 wt%) than LG and ZB. Derivative plots for RW and WW show the presence of shoulder indicating the presence of hemicellulose-cellulose structures. The results provided in Figs. 4 and 5 show that the lignocellulosic biomass feedstocks used in this study can be divided into three categories: (i) high hemicellulose-cellulose, lower cellulose-lignin structures, (ii) low hemicellulose-cellulose, higher cellulose-lignin structures, (iii) cellulose-lignin only structures.

3.3. Thermal analysis of the hydrochars

3.3.1. High hemicellulose-cellulose, low cellulose-lignin structures (CR)

Fig. 6 shows the proximate analysis of hydrochars (or solid residues) produced by the hydrothermal conversion of CR. The higher temperatures produce a higher ratio of VM and a lower ratio of FC compared to raw CR, which results in lower fuel ratios at higher temperatures (Fig. 6). Furthermore, the ash content of hydrochars increased consistently particularly at high pressures.

Fig. 7 presents the derivative weight loss rates of raw and hydrochars produced by the hydrothermal process of CR and the displacement at the process conditions. The degree of displacement relates directly to process temperature and pressure. Despite the noise in the weight loss rates at 250 °C (in Fig. 7a-c), there is a remarkable difference between the thermal decomposition profiles of the hydrochars produced at different conditions.

The hydrochars produced at lower temperatures (75 °C and 150 °C)

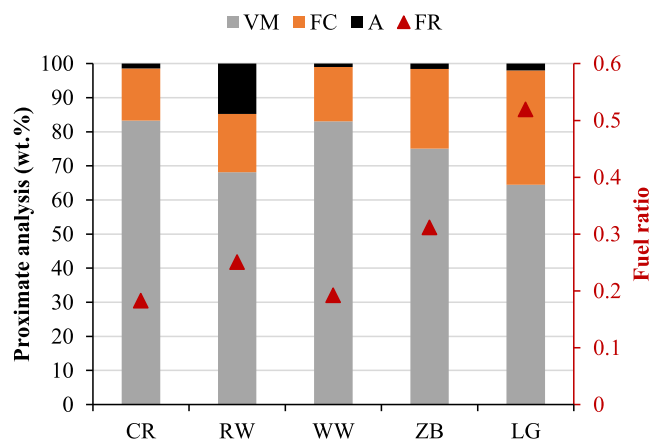


Fig. 3. Proximate analysis (dry basis), fuel ratio (FR) of raw biomasses (CR-Coffee residue, RW-Rice waste, WW-White wood, ZB- Zilkha black, LG-Lignin).

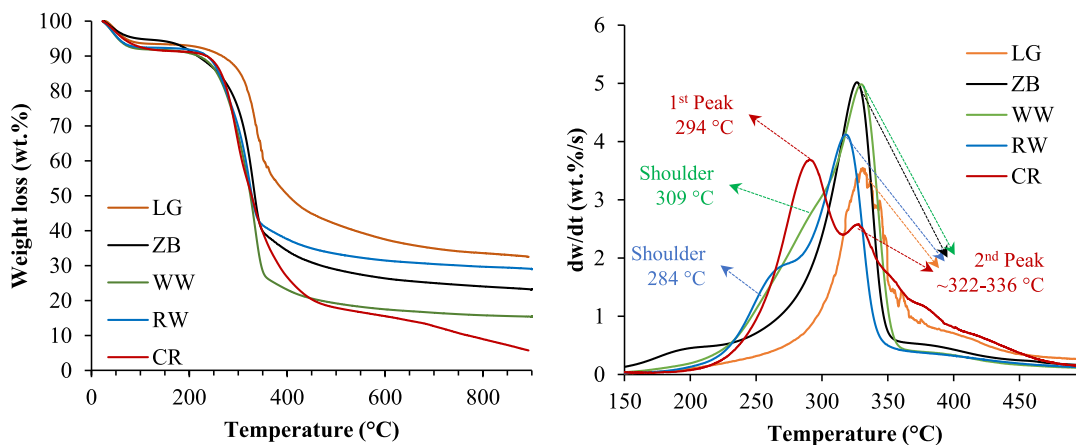


Fig. 4. Weight loss and weight loss rates of the raw biomasses in slow pyrolysis (CR-Coffee residue, RW-Rice waste, WW-White wood, ZB- Zilkha black, LG-Lignin).

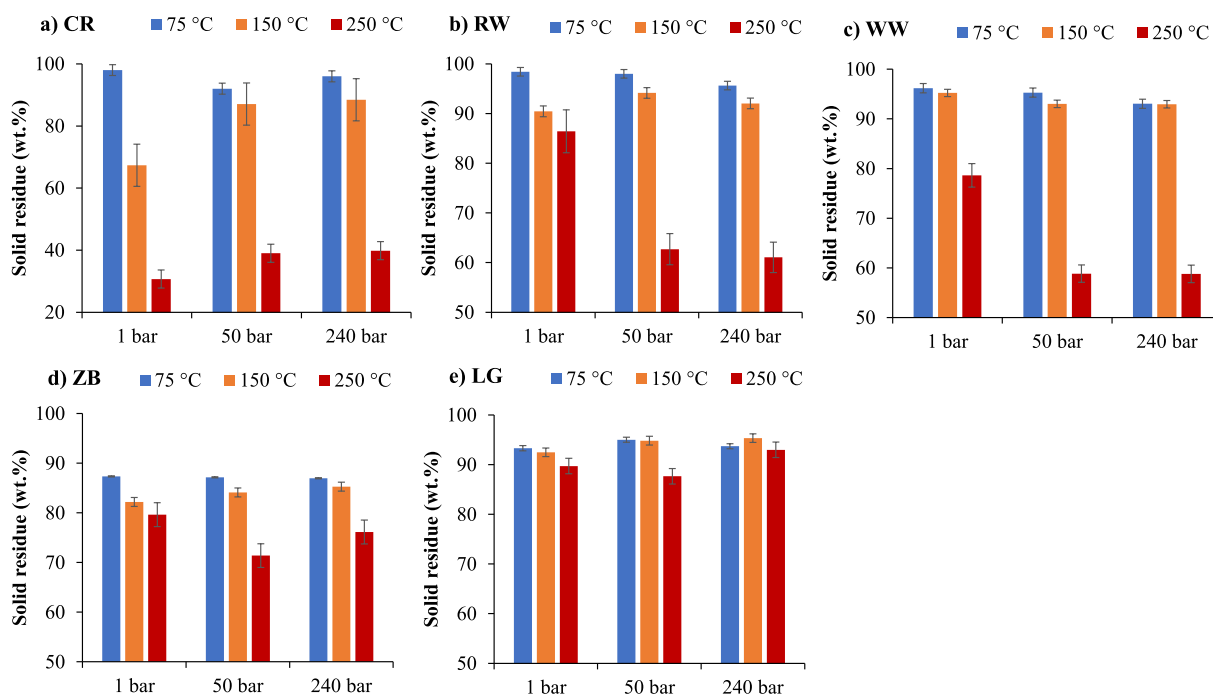


Fig. 5. Solid residue (hydrochar) yields of biomasses; a) CR, b) RW, c) WW, and d) ZB and e) LG after the hydrothermal treatment at 75, 150, 250 °C and 1, 50, 240 bar.

provides two characteristic weight loss rate peaks at ~ 290 °C and ~ 330 °C, which has the similar weight loss rates compare with the CR feedstock. Additionally, the displacements at these temperatures do not demonstrate a significant difference as shown in Fig. 7d. However, hydrothermal conversion of CR at 250 °C produces a hydrochar with a single thermal decomposition peak at ~ 340 – 350 °C (Fig. 7a-c) due to the cellulose-lignin only structures remaining after the hydrothermal treatment. Hemicellulose appears to have fully solubilized into the water at a temperature above ~ 160 °C, effectively under subcritical water conditions [25]. Since the hemicellulose is an amorphous heteropolysaccharide present as approximately 20–30 wt% of the dry weight of most wood species. Hemicellulose forms hydrogen bonds with cellulose and covalent bonds with lignin (primarily α -benzyl ether bonds), and ester bonds with hydroxycinnamic acids and acetyl units [45]. The different bonding in hemicellulose compared to cellulose, together with differences in crystallinity and molecular weight mean that the hemicellulose is more easily degraded under hydrothermal treatment, as seen in Fig. 7a-c. The first peak disappeared due to a complete degradation of

the hemicellulose structures from the CR at 250 °C, 1240 bar. The hydrochars produced at 250 °C, therefore, presents a mixture of low cellulose-high lignin structures, which could result in a higher heating value as lignin has a higher heating value than hemicellulose and cellulose [46]. The weight loss rate was 7.3, 4.5, and 6.0 wt.%/s at 250 °C and pressures of 1, 50, and 240 bar. Hydrochars produced at 250 °C, therefore, demonstrate a greater displacement ~ 5000 – 7000 as seen in Fig. 7d.

3.3.2. Lower hemicellulose-cellulose, higher cellulose-lignin structures (RW and WW)

The proximate analysis of hydrochars (or solid residues) produced by the hydrothermal conversion of the biomasses having lower hemicellulose-cellulose and higher cellulose-lignin structures (RW and WW) are presented in Fig. 8. Although there is a clear difference in ash content between RW and WW, these two lignocellulosic biomasses show similar levels of thermal decomposition, as a result of their similar hemicellulose, cellulose, and lignin compositions. RW and WW produce

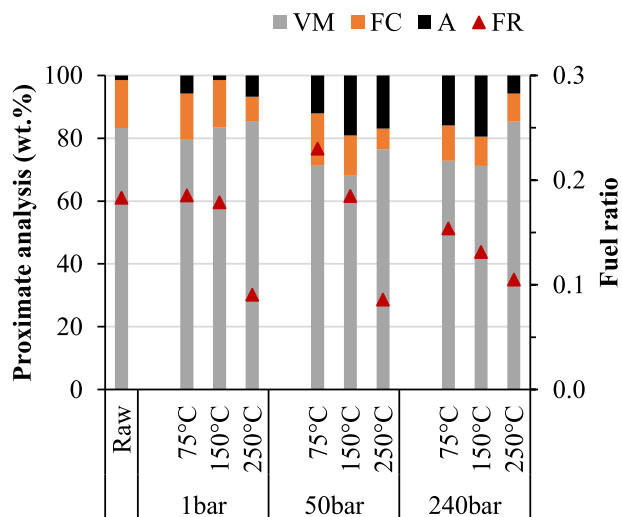


Fig. 6. Proximate analysis (dry basis) of CR and hydrochars produced at the temperatures of 75–250 °C under the pressure of 1–240 bar. VM – Volatile Matter (db) FC – Fixed Carbon (db) A – Ash (db) FR – Fuel Ratio (dafb).

a hydrochar with a higher volatile matter and lower fixed carbon contents compared to untreated RW (Fig. 8a) and WW (Fig. 8b). RW has the highest ash content (~15 wt%) compared with the other biomass feedstocks and the ash content does not change significantly after the hydrothermal treatment. RW ash is predominantly SiO₂ based and

insoluble under hydrothermal conditions [47]. Pressure has no effect on the proximate composition of the hydrochars. At 250 °C there is an apparent increase in volatile content as a result of the removal of the hemicellulose component, (based on Fig. 9a-c) which is not possible at lower temperatures without acid/alkali addition [48]. This increase is only relative to the overall composition of the biochar and caused by the insolubility of the SiO₂ in the RW and the increased solubility of the hemicellulose fraction at 250 °C.

The weight-loss rates and the displacements of RW and WW hydrochars are presented in Fig. 9 and Fig. 10, respectively. The thermal decomposition of RW hydrochars show a small detectable shift from 322 °C to 333–340 °C as seen in Fig. 9a-c. The hydrochars produced at lower temperatures (75 °C and 150 °C) provides similar trends with the raw RW, a strong peak at ~ 333 °C with a weight loss rate of ~ 5.2 wt. %/s, (cellulose-lignin) and a shoulder at lower temperatures of ~ 304 °C (hemicellulose-cellulose) of 2.3 wt.%/s (Fig. 9a-c). The hemicellulose-cellulose levels in RW and WW are much lower than in CR. Therefore, it appears as a peak in the decomposition of CR (Fig. 7ac) while it is only a shoulder in the decomposition of RW (Fig. 9a-c) and WW (Fig. 10a-c). The hemicellulose and cellulose structures were degraded and solubilised above ~ 160 °C and ~ 220 °C, respectively, under subcritical water conditions [25,44] due to the catalytic effect of hydroxyl (OH⁻) and hydronium (H⁺) ions. The shoulder (hemicellulose-cellulose) disappeared at 250 °C and 50–240 bar. The displacement (Fig. 9d) also demonstrates the similarity with the thermal decomposition of the solid residues at low temperatures (75 °C and 150 °C) and changes seen at higher temperatures (250 °C). Neither pressure nor temperature has a significant effect on the solid residues produced at lower temperatures

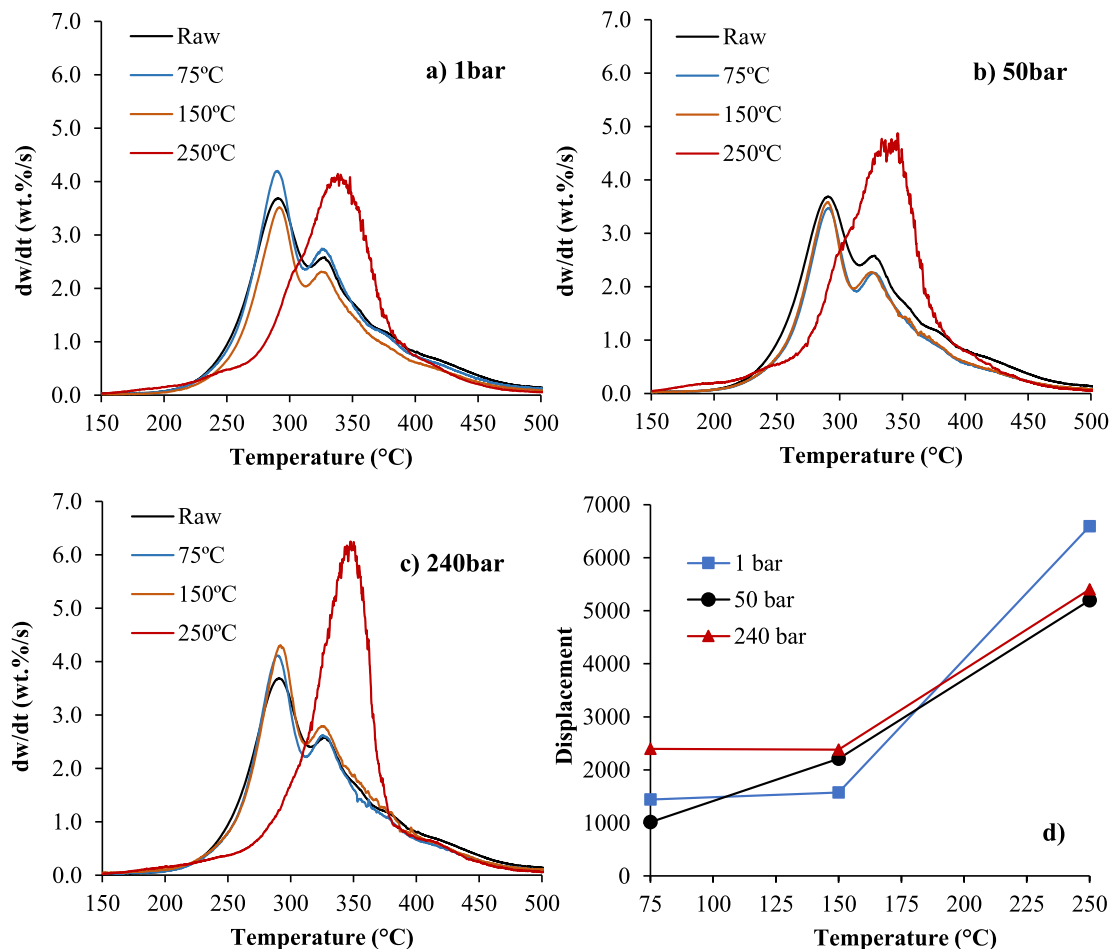


Fig. 7. Weight-loss rates of raw and hydrochars (or solid residues) produced by the hydrothermal treatment of CR at a)1 bar, b) 50 bar, c) 240 bar and d) displacement at the hydrothermal process conditions.

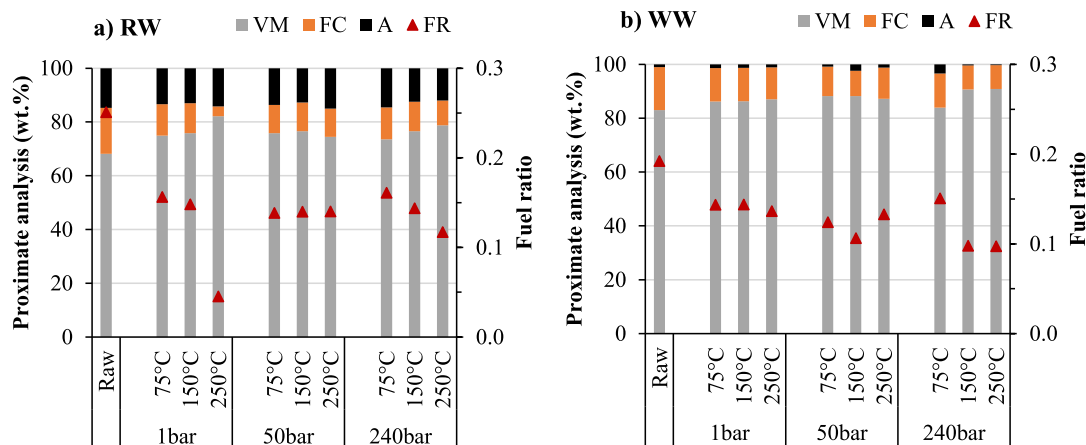


Fig. 8. Proximate analysis (dry basis) of a) RW hydrochars and b) WW hydrochars produced at the temperatures of 75–250 °C under the pressure of 1–240 bar. VM – Volatile Matter (db) FC – Fixed Carbon (db) A – Ash (db) FR – Fuel Ratio (dafb).

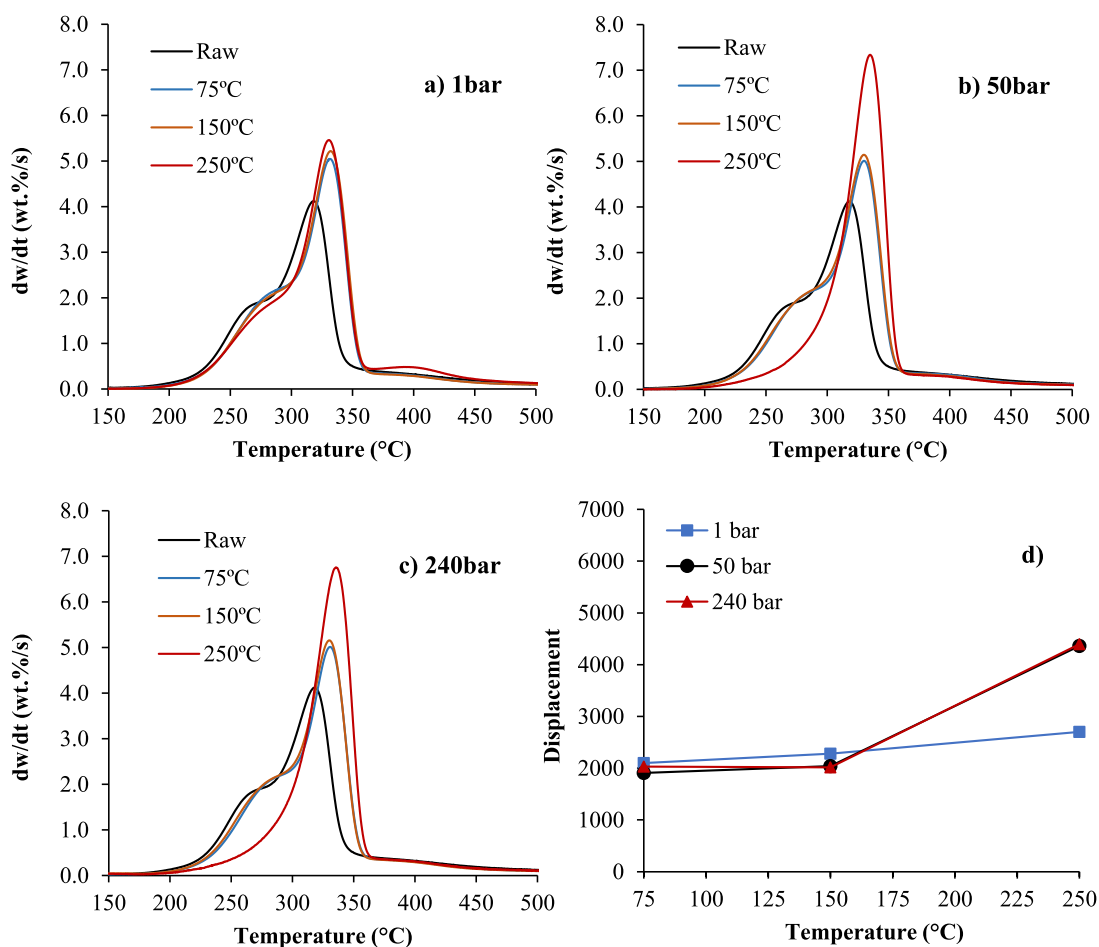


Fig. 9. Weight-loss rates of raw and hydrochars (or solid residues) produced by the hydrothermal process of RW at a) 1 bar, b) 50 bar, c) 240 bar and d) displacement at the hydrothermal process conditions.

(75 °C and 150 °C), while a significant difference was observed for the hydrochars produced at higher temperatures of 250 °C. The WW hydrochar derivative plots also show a shift to the higher temperature from 333 °C to 340 °C at 1 bar (Fig. 10a) and a further shift to ~ 350 °C at 50 bar and 240 bar (Fig. 10b and 10c). The weight-loss rates are ~ 6.0 wt.%/s at low hydrothermal temperatures (75 °C and 150 °C) and increased to ~ 6.8 wt.%/s with the temperature increase to 250 °C at 1 bar. The hydrochars produced at 75 °C and 150 °C indicate the shoulders

which indicate the presence of hemicellulose-cellulose structures. However, the shoulder disappeared at 250 °C, at 50 bar and 240 bar (Fig. 10a-c), which is characteristically similar to RW.

3.3.3. High cellulose-lignin structures (ZB and LG)

Fig. 11 shows the proximate analysis of the hydrochars produced by the ZB and LG, which have a high level of cellulose-lignin structures. These biomasses (ZB and LG) are defined as having higher FC and lower

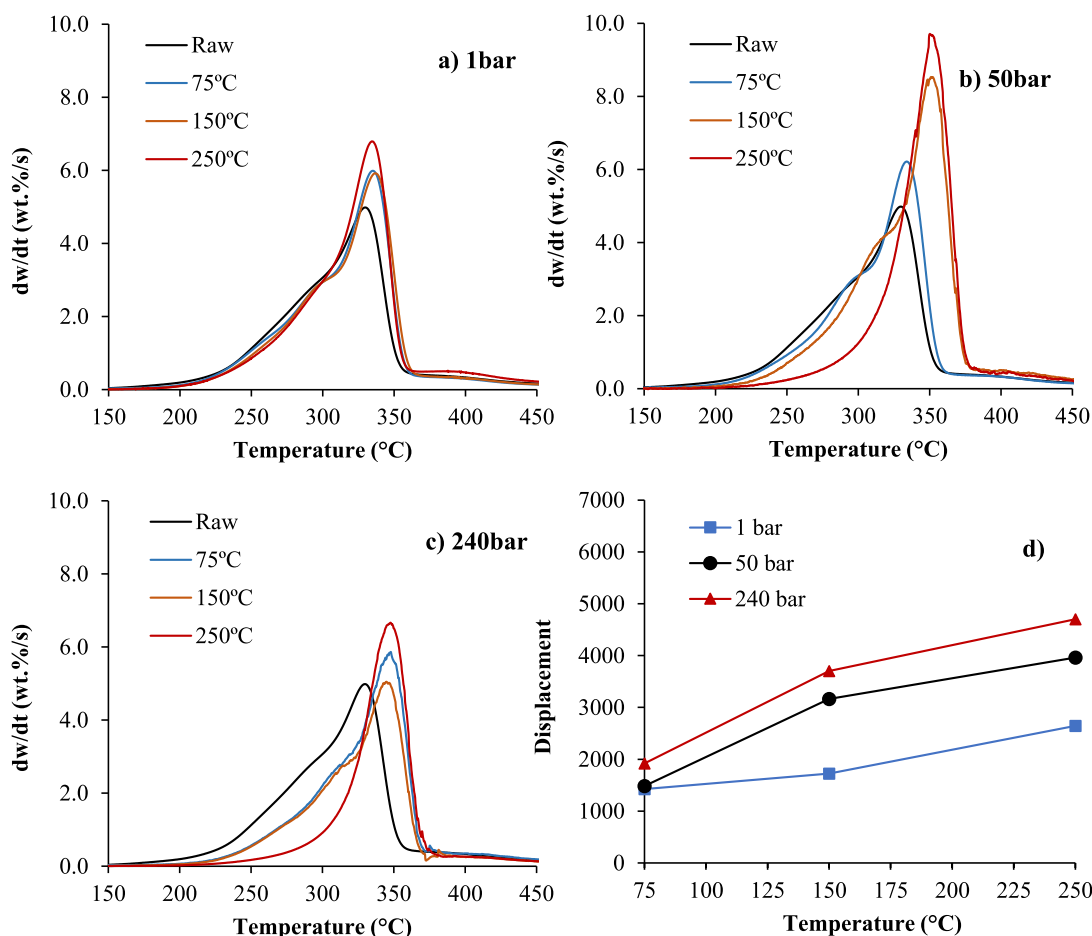


Fig. 10. Weight-loss rates of raw and hydrochars (or solid residues) produced by the hydrothermal process of WW at a) 1 bar, b) 50 bar, c) 240 bar and d) displacement at the hydrothermal process conditions.

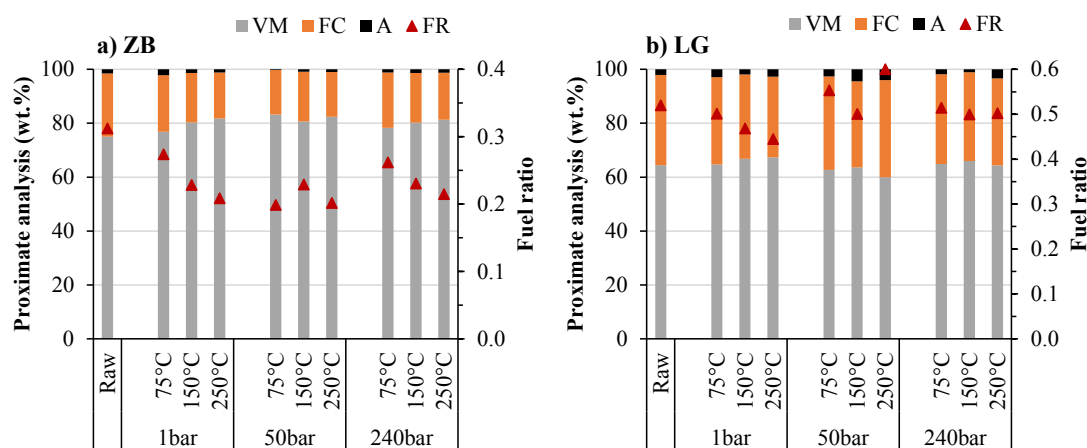


Fig. 11. Proximate analysis (dry basis) of a) ZB hydrochars and b) LG hydrochars produced at the temperatures of 75–250 $^{\circ}C$ under the pressure of 1–240 bar. VM – Volatile Matter (db) FC – Fixed Carbon (db) A – Ash (db) FR – Fuel Ratio (dafb).

VM compare to other biomasses, which results in higher fuel ratio and potentially higher heating value due to higher levels of lignin. The proximate composition of these two biomass types show insignificant changes during hydrothermal treatment at 75–250 $^{\circ}C$. The small differences could be therefore attributed to the absence of hemicellulose structures which usually decompose at \sim 180–200 $^{\circ}C$.

The thermal decomposition of the ZB and LG provides only one peak at \sim 330 $^{\circ}C$, indicating that minimal hemicellulose is present. The

thermal decomposition of the hydrochars produced by ZB shows a slight shift to a higher temperature of \sim 336 $^{\circ}C$ (Fig. 12); however, the hydrochars produced by LG provide similar thermal decomposition profiles compare with the LG (Fig. 13). The slight shift in the ZB hydrochars could be attributed to the decomposition of cellulose. However, LG hydrochars have cellulosic material and therefore did not provide any shift in the thermal decomposition, proving that neither pressure nor temperature had a significant effect on hydrochars

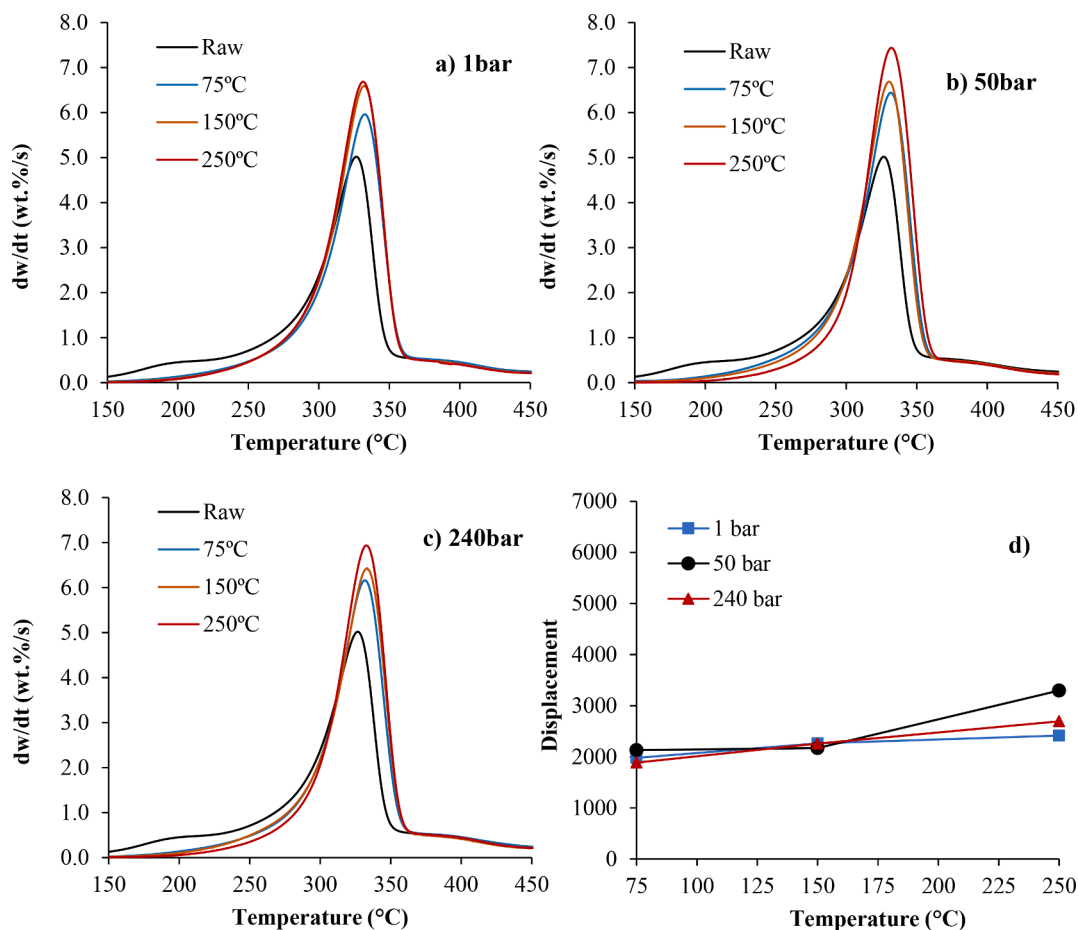


Fig. 12. Weight-loss rates of raw and hydrochars (or solid residues) produced by the hydrothermal process of ZB at a) 1 bar, b) 50 bar, c) 240 bar and d) displacement at the hydrothermal process conditions.

generated from biomass with a high lignin content (Fig. 13). The weight-loss rates of ZB hydrochars are ~ 6 – 8 wt.%/s when treated at > 75 °C and do not show any significant change as pressure changes, as shown in Fig. 12. However, the LG hydrochars show little difference in weight loss rates at any temperature or pressure, as shown in Fig. 13. Unlike CR, WW, RW, ZB and LG both produce minimal displacements (Fig. 12d and 13d) during hydrothermal conversion, which can be attributed to the high levels of lignin in ZB and LG. Lignin is an amorphous natural polymer made up of aromatic blocks which are cross-linked by carbon and ether linkages and considered to be hydrophobic due to its low solubility in water.

3.4. Relationship between char yield and displacement

Fig. 14 shows the relationship between char yield and displacement at the specific temperature and pressure conditions of hydrothermal treatment. The differences in the relationship between char yield and displacement of the biomass categories were clearly demonstrated in Fig. 14. Hydrochars produced at lower temperatures (< 150 °C) show relatively small displacements while the hydrochars produced at higher temperature (200 °C) showed relatively higher displacement.

The highest decomposition and displacement were observed for category (i) biomass feedstocks (CR (red bubbles)) at 250 °C at all pressures. Category (ii) biomass feedstocks (RW (blue bubbles) and WW (green bubbles)) demonstrated the second highest decomposition and displacement, as both hemicellulose and cellulose structures in category (i) and (ii) were successfully degraded under subcritical conditions. The robust lignin structures in category (iii) biomass feedstocks (ZB (black bubbles) and LG (orange bubbles)) resulted in the lowest decomposition

and displacement at any temperature and pressure of hydrothermal treatment compared to other two categories. The increase in pressure slightly increases the displacement level of the biomasses at a low temperature (75 °C and 150 °C).

4. Conclusions

This study explored the hydrothermal treatment of biomass in a semi-continuous flow rig. The solid residues at < 150 °C and < 240 bar did not show any significant structural changes compared with the untreated biomass feedstocks. However, the hydrochars produced at 250 °C and 50–240 bar demonstrates significant structural modifications depending on the biomass type. The first category provided relatively low hydrochar yield (~ 39 wt%) due to the degradation of higher hemicellulose-cellulose structures. The second category demonstrated relatively higher hydrochar yields (58–62 wt%) compared to (i). Category (iii) had the highest hydrochar yields (~ 73 wt% for ZB and ~ 90 wt% for LG) due to the absence of hemicellulose and generally lower cellulose. The novel displacement analysis method produced a similar trend. Biomass with a higher hemicellulose content produced the highest levels of displacement, with the least displacements resulting from the highest lignin samples. The “displacement” method could thus be a new characterisation technique for the hydrochars to show the quantitative impact of hydrothermal treatment.

CRedit authorship contribution statement

Fatih Güleş: Conceptualization, Formal analysis, Investigation, Validation, Visualization, Writing - original draft, Writing - review &

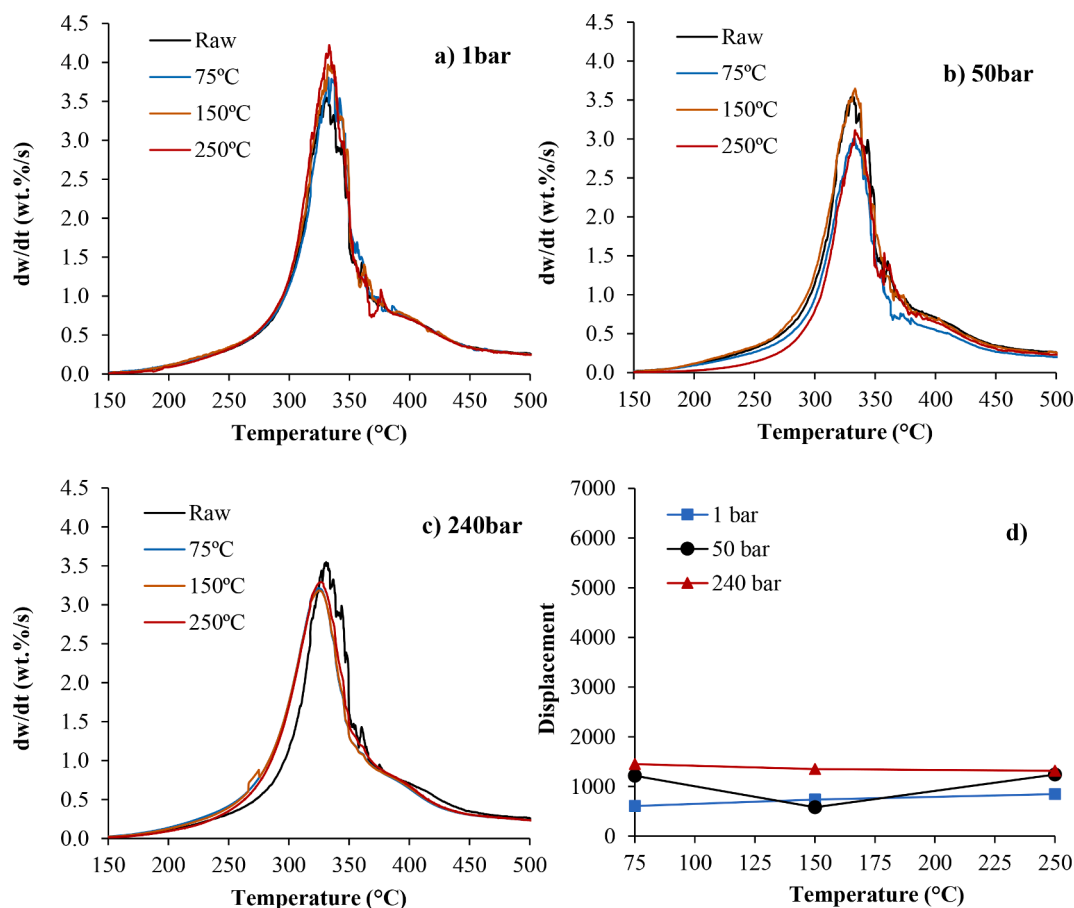


Fig. 13. Weight-loss rates of raw and hydrochars (or solid residues) produced by the hydrothermal process of LG at a) 1 bar, b) 50 bar, c) 240 bar and d) displacement at the hydrothermal process conditions.

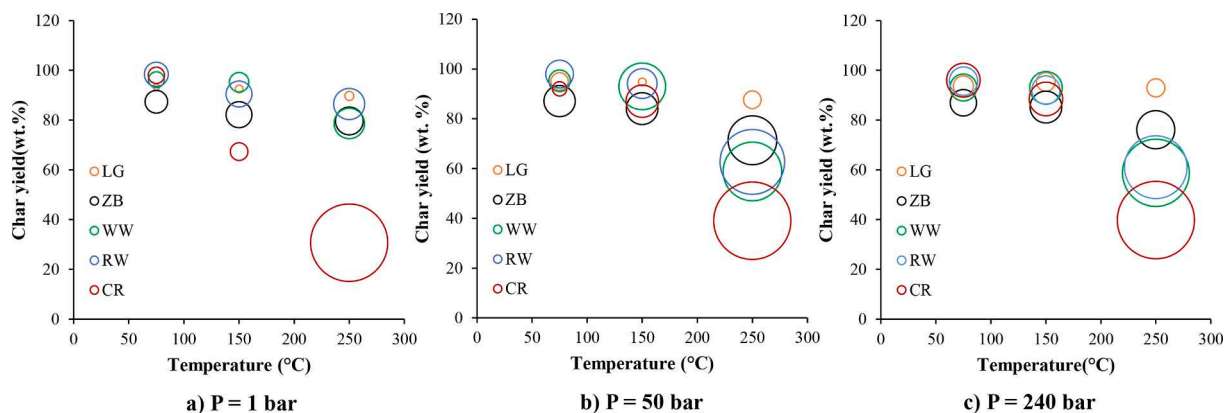


Fig. 14. Relationship between char yield and displacement values under the hydrothermal treatment conditions. The width of bubbles represents the displacement value at each temperature (x axis, 75, 150, 250 °C) and pressure (a) 1 bar, b) 50 bar, c) 240 bar).

editing. **Luis Miguel Garcia Riesco:** Investigation, Methodology, Formal analysis. **Orla Williams:** Conceptualization, Formal analysis, Supervision, Writing - review & editing. **Emily T. Kostas:** Methodology, Formal analysis, Writing - review & editing. **Abby Samson:** Methodology, Formal analysis, Writing - review & editing. **Edward Lester:** Conceptualization, Methodology, Formal analysis, Supervision, Project administration, Funding acquisition, Visualization, Writing - review & editing.

Declaration of Competing Interest

The authors declare that they have no known competing financial interests or personal relationships that could have appeared to influence the work reported in this paper.

Acknowledgement

This research was funded and supported by the EPSRC & BBSRC UK Supergen Bioenergy Hub [Grant number EP/S000771/1].

References

- [1] Lester E, Avila C, Pang CH, Williams O, Perkins J, Gaddipatti S, et al. A proposed biomass char classification system. *Fuel* 2018;232:845–54.
- [2] Shen Y. A review on hydrothermal carbonization of biomass and plastic wastes to energy products. *Biomass Bioenergy* 2020;134.
- [3] Sharma R, Jasrotia K, Singh N, Ghosh P, Srivastava S, Sharma NR, et al. A Comprehensive Review on Hydrothermal Carbonization of Biomass and its Applications. *Chemistry. Africa* 2019;3(1):1–19.
- [4] Daioglou V, Doelman JC, Wicke B, Faaij A, van Vuuren DP. Integrated assessment of biomass supply and demand in climate change mitigation scenarios. *Global Environ Change* 2019;54:88–101.
- [5] Guo M, Song W. The growing US bioeconomy: Drivers, development and constraints. *New Biotechnol* 2019;49:48–57.
- [6] Williams O, Newbolt G, Eastwick C, Kingman S, Giddings D, Lormor S, et al. Influence of mill type on densified biomass comminution. *Appl Energy* 2016;182: 219–31.
- [7] Williams O, Eastwick C, Kingman S, Giddings D, Lormor S, Lester E. Investigation into the applicability of Bond Work Index (BWI) and Hardgrove Grindability Index (HGI) tests for several biomasses compared to Colombian La Loma coal. *Fuel* 2015; 158:379–87.
- [8] Vassilev SV, Vassileva CG, Vassilev VS. Advantages and disadvantages of composition and properties of biomass in comparison with coal: An overview. *Fuel* 2015;158:330–50.
- [9] Isikgor FH, Becer CR. Lignocellulosic biomass: a sustainable platform for the production of bio-based chemicals and polymers. *Polym Chem* 2015;6(25): 4497–559.
- [10] Antero RVP, Alves ACF, de Oliveira SB, Ojala SA, Brum SS. Challenges and alternatives for the adequacy of hydrothermal carbonization of lignocellulosic biomass in cleaner production systems: A review. *J Cleaner Prod* 2020;252.
- [11] Wang S, Dai G, Yang H, Luo Z. Lignocellulosic biomass pyrolysis mechanism: a state-of-the-art review. *Prog Energy Combust Sci* 2017;62:33–86.
- [12] Ruiz HA, Rodríguez-Jasso RM, Fernandes BD, Vicente AA, Teixeira JA. Hydrothermal processing, as an alternative for upgrading agriculture residues and marine biomass according to the biorefinery concept: a review. *Renew Sustain Energy Rev* 2013;21:35–51.
- [13] Pedersen TH, Grigoras I, Hoffmann J, Toor SS, Daraban IM, Jensen CU, et al. Continuous hydrothermal co-liquefaction of aspen wood and glycerol with water phase recirculation. *Appl Energy* 2016;162:1034–41.
- [14] Kumar M, Oyedun AO, Kumar A. A review on the current status of various hydrothermal technologies on biomass feedstock. *Renew Sustain Energy Rev* 2018; 81:1742–70.
- [15] Cherad R, Onwudili J, Biller P, Williams P, Ross A. Hydrogen production from the catalytic supercritical water gasification of process water generated from hydrothermal liquefaction of microalgae. *Fuel* 2016;166:24–8.
- [16] Abdoulmoumine N, Adhikari S, Kulkarni A, Chattanathan S. A review on biomass gasification syngas cleanup. *Appl Energy* 2015;155:294–307.
- [17] Elliott DC, Biller P, Ross AB, Schmidt AJ, Jones SB. Hydrothermal liquefaction of biomass: developments from batch to continuous process. *Bioresour Technol* 2015; 178:147–56.
- [18] Dimitriadis A, Bezergianni S. Hydrothermal liquefaction of various biomass and waste feedstocks for biocrude production: A state of the art review. *Renew Sustain Energy Rev* 2017;68:113–25.
- [19] Şimşek EH, Güleç F, Akçadağ FS. Understanding the liquefaction mechanism of Beypazarı lignite in tetralin with ultraviolet irradiation using discrete time models. *Fuel Process Technol* 2020;198:106227.
- [20] Güleç F, Özdemir GDT. Investigation of drying characteristics of Cherry Laurel (*Laurocerasus officinalis* Roemer) fruits. *Akademik ziraat dergisi* 2017;6(1):73–80.
- [21] Heidari M, Norouzi O, Salaudeen S, Acharya B, Dutta A. Prediction of Hydrothermal Carbonization with Respect to the Biomass Components and Severity Factor. *Energy Fuels* 2019;33(10):9916–24.
- [22] Arellano O, Flores M, Guerra J, Hidalgo A, Rojas D, Strubinger A. Hydrothermal carbonization (HTC) of corncob and characterization of the obtained hydrochar. *Chem Eng* 2016;50.
- [23] Wei L, Sevilla M, Fuertes AB, Mokaya R, Yushin G. Hydrothermal carbonization of abundant renewable natural organic chemicals for high-performance supercapacitor electrodes. *Adv Energy Mater* 2011;1(3):356–61.
- [24] Álvarez-Murillo A, Sabio E, Ledesma B, Román S, González-García C. Generation of biofuel from hydrothermal carbonization of cellulose. Kinetics modelling. *Energy* 2016;94:600–8.
- [25] Heidari M, Dutta A, Acharya B, Mahmud S. A review of the current knowledge and challenges of hydrothermal carbonization for biomass conversion. *J Energy Inst* 2019;92(6):1779–99.
- [26] Kambo HS, Dutta A. Strength, storage, and combustion characteristics of densified lignocellulosic biomass produced via torrefaction and hydrothermal carbonization. *Appl Energy* 2014;135:182–91.
- [27] Subedi R, Kammann C, Pelissetti S, Sacco D, Grignani C, Monaco S. Recycling of organic residues for agriculture: from waste management to ecosystem services. 15th International Conference RAMIRAN. 2013.
- [28] Guangzhi Y, Jinyu Y, Yuhua Y, Zhihong T, DengGuang Y, Junhe Y. Preparation and CO₂ adsorption properties of porous carbon from camphor leaves by hydrothermal carbonization and sequential potassium hydroxide activation. *RSC Adv* 2017;7(7): 4152–60.
- [29] Liu Z, Zhang F, Hoekman SK, Liu T, Gai C, Peng N. Homogeneously dispersed zerovalent iron nanoparticles supported on hydrochar-derived porous carbon: simple, in situ synthesis and use for dechlorination of PCBs. *ACS Sustainable Chem Eng* 2016;4(6):3261–7.
- [30] Fan F, Xing X, Shi S, Zhang X, Zhang X, Li Y, et al. Combustion characteristic and kinetics analysis of hydrochars. *Transactions of the Chinese Society of Agricultural Engineering* 2016;32(15):219–24.
- [31] Hao W, Björkman E, Lilliestråle M, Hedin N. Activated carbons for water treatment prepared by phosphoric acid activation of hydrothermally treated beer waste. *Ind Eng Chem Res* 2014;53(40):15389–97.
- [32] Titirici M-M, Antonietti M, Baccile N. Hydrothermal carbon from biomass: a comparison of the local structure from poly- to monosaccharides and pentoses/hexoses. *Green Chem* 2008;10(11):1204–12.
- [33] Lester E, Gong M, Thompson A. A method for source apportionment in biomass/coal blends using thermogravimetric analysis. *J Anal Appl Pyrol* 2007;80(1): 111–7.
- [34] Kostas ET, Williams OS, Duran-Jimenez G, Tapper AJ, Cooper M, Meehan R, et al. Microwave pyrolysis of *Laminaria digitata* to produce unique seaweed-derived bio-oils. *Biomass Bioenergy* 2019;125:41–9.
- [35] Kostas ET, White DA, Cook DJ. Development of a bio-refinery process for the production of speciality chemical, biofuel and bioactive compounds from *Laminaria digitata*. *Algal research* 2017;28:211–9.
- [36] Paczkowski S, Sauer C, Anetzberger A, Paczkowska M, Russ M, Wöhler M, et al. Feedstock particle size distribution and water content dynamic in a pellet mill production process and comparative sieving performance of horizontal 3.15-mm mesh and 3.15-mm hole sieves. *Biomass Convers Biorefin* 2019:1–12.
- [37] DIN Deutsches Institut für Normung 2016.
- [38] Koechermann J, Goersch K, Wirth B, Muehlenberg J, Klemm M. Hydrothermal carbonization: Temperature influence on hydrochar and aqueous phase composition during process water recirculation. *J Environ Chem Eng* 2018;6(4): 5481–7.
- [39] Ninduangdee P, Kuprianov VI, Cha EY, Kaewrath R, Youngyuen P, Athawethworawuth W. Thermogravimetric studies of oil palm empty fruit bunch and palm kernel shell: TG/DTG analysis and modeling. *Energy Procedia* 2015;79: 453–8.
- [40] Pang CH, Gaddipatti S, Tucker G, Lester E, Wu T. Relationship between thermal behaviour of lignocellulosic components and properties of biomass. *Bioresour Technol* 2014;172:312–20.
- [41] Gollakota AR, Reddy M, Subramanyam MD, Kishore N. A review on the upgradation techniques of pyrolysis oil. *Renew Sustain Energy Rev* 2016;58: 1543–68.
- [42] Carrier M, Auret L, Bridgwater A, Knoetze JH. Using apparent activation energy as a reactivity criterion for biomass pyrolysis. *Energy Fuels* 2016;30(10):7834–41.
- [43] Yang H, Yan R, Chen H, Lee DH, Zheng C. Characteristics of hemicellulose, cellulose and lignin pyrolysis. *Fuel* 2007;86(12–13):1781–8.
- [44] Tekin K, Karagöz S, Bektaş S. A review of hydrothermal biomass processing. *Renew Sustain Energy Rev* 2014;40:673–87.
- [45] Ren J, Sun R. Hemicelluloses. *Cereal straw as a resource for sustainable biomaterials and biofuels* Amsterdam: Elsevier; 2010. p. 73–130.
- [46] Vassilev SV, Baxter D, Andersen LK, Vassileva CG, Morgan TJ. An overview of the organic and inorganic phase composition of biomass. *Fuel* 2012;94:1–33.
- [47] Ludueña LN, Fasce DP, Alvarez VA, Stefani PM. Nanocellulose from rice husk following alkaline treatment to remove silica. *Bioresour* 2011;6(2):1440–53.
- [48] Barana D, Salanti A, Orlandi M, Ali DS, Zoia L. Biorefinery process for the simultaneous recovery of lignin, hemicelluloses, cellulose nanocrystals and silica from rice husk and *Arundo donax*. *Ind Crops Prod* 2016;86:31–9.